

## **Mixed-layer simulations at OWS Bravo: the role of salinity in interannual variability of the upper ocean at high latitude**

**C.L. Tang<sup>1</sup>, S.J.D. D'Alessio<sup>2\*</sup> and B.M. DeTracey<sup>1</sup>**

<sup>1</sup>*Bedford Institute of Oceanography,  
Ocean Sciences Division  
Department of Fisheries and Oceans,  
Dartmouth, Nova Scotia, Canada B2Y 4A2*

<sup>2\*</sup>*Department of Applied Mathematics,  
University of Waterloo, Waterloo,  
Ontario, Canada N2L 3G1  
Email: [sdalessio@uwaterloo.ca](mailto:sdalessio@uwaterloo.ca)*

### **Abstract**

The role of salinity in mixed layer dynamics is investigated at the high latitude location of ocean weather ship station (OWS) Bravo. To accomplish this two common types of one-dimensional mixed-layer models were employed during two periods exhibiting significantly different oceanographic conditions. In the mixed-layer simulations the salinity is prescribed according to existing data. Depending how the salinity is specified, good agreement between simulated and observed SST can be achieved. A comparison of the different methods used to specify salinity reveals that the simulated SST and mixed-layer depths are particularly sensitive to changes in salinity, especially during the cooling phase. This is because density changes are generally more sensitive to salinity at high latitudes. Model simulations are carried out during the period 1964-1965 as well as during the period 1969-1971. The 1964-1965 period is one having normal salinity while the 1969-1971 period is characterized as having abnormally low salinity and mild winters. A thorough comparison of the model simulations during these two periods indicates that the low surface salinity, and not the reduced surface cooling during 1969-1971, is mainly responsible for the shallow depth of the mixed-layer during that period. Furthermore, the smaller surface heat loss during 1969-1971 does not result in a higher winter sea-surface temperature as expected due to the low entrainment rate during this period. The model results suggest that salinity can be as important as the surface heat flux in controlling the interannual variation of the mixed layer depth at OWS Bravo.

**Keywords:** mixed-layer simulations, OWS Bravo, role of salinity, Labrador Sea.

## Introduction

The mixed-layer temperature and depth are controlled mainly by: (1) air-sea interaction, i.e., surface buoyancy flux and wind mixing; (2) the stability of the water column; (3) the internal dynamics of the mixed layer; (4) turbulent entrainment at the base of the mixed layer. At locations with strong currents, or strong horizontal gradients in temperature or salinity, advection is also important. Wind mixing and buoyancy losses from the upper ocean by air-sea fluxes can increase the mixed-layer depth, while increases in buoyancy can decrease the mixed-layer depth. The stability of the water column, i.e. vertical stratification, is controlled by both the air-sea interaction and advection. A highly-stratified upper ocean inhibits the development of deep mixed layers, while a weakly-stratified upper ocean, on the other hand, favors deep convection. Due to the different mean water temperature and the non-linear dependence of density on temperature and salinity, vertical density changes / stability, and thus, the mixed-layer temperature and depth at high latitudes are generally more sensitive to salinity than those at low- and mid-latitudes. To illustrate this point, we computed the contributions of temperature and salinity to density change for ocean weather ship stations (OWS) November ("N"), Papa ("P") and Bravo ("B") separately. The ranges of the seasonal temperature and salinity variations at these three locations are shown on a common  $T$ - $S$  plane in Figure 1. The change in density,  $\Delta\rho$ , at a given pressure can be approximated as the sum of two terms corresponding to changes in  $T$  and  $S$ :

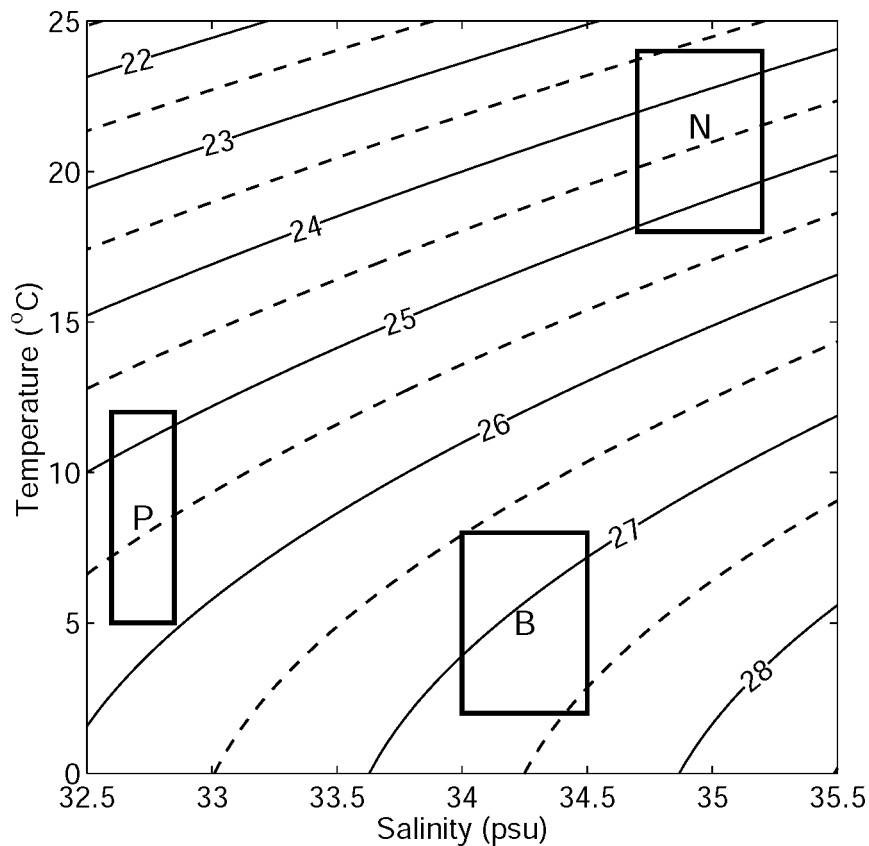


**Figure 1:** Mixed-layer temperature and salinity during March-April for OWS November (N) (140°W, 30°N), OWS Papa (P) (145°W, 50°N) and OWS Bravo (B) (56.5°W, 56°W) in the temperature-salinity plane. The solid and dotted lines are density contours (actual density – 1000 in units of kilograms per cubic meter).

$$\Delta\rho = \frac{\partial\rho}{\partial T}\Delta T + \frac{\partial\rho}{\partial S}\Delta S,$$

where  $\Delta T$  and  $\Delta S$  are the ranges of  $T$  and  $S$  shown in Figure 1. The ratio of the first to the second term on the right-hand-side of this equation is 1: 0.16 at Papa, 1: 0.22 at November, and 1: 0.57 at Bravo. The significantly larger ratio at Bravo indicates that salinity contributes more to the density change at Bravo than it does at Papa and November.

The mixed-layer depth and temperature at Papa and November have been shown to be weakly dependent on salinity (e.g., [1] – [3]). In previous model simulations, a constant salinity or salinity profiles based on climatology were used. The salinity profiles were either taken to be independent of time or used as an initial condition with and without a surface water flux.

The main objective of this paper is to investigate the role of salinity in the mixed-layer dynamics in the central Labrador Sea using data from OWS Bravo (56.5°N, 51°W) and two mixed-layer models. Shown in Figure 2 is the location and the local bathymetry of OWS Bravo. The model sensitivity to salinity will be investigated by employing different methods of specifying the salinity in the models. Since the surface heat flux is a major process influencing the mixed-layer depth and temperature, we will assess the relative contributions of salinity and heat flux to the mixed-layer variability by comparing the mixed-layer depth and temperature during two periods in the 1960s and 1970s that have different oceanographic and atmospheric conditions.

The relationship between the heat flux, stratification, and mixed-layer temperature and depth is not always straightforward; simple arguments may be inadequate to explain all the observations because of the competing oceanic processes at work. For example, intense cooling during a cold winter can lower the mixed-layer temperature, but it can also create a deep mixed layer and entrain more warm water into the mixed layer, that increases the mixed-layer temperature. Whether the resulting mixed-layer temperature is above or below average in this example will depend on the relative contributions of these two processes. Mixed-layer models can simulate both processes and can provide quantitative results to explain the mixed-layer depth and temperature.

The paper is structured as follows. The subsequent section introduces the governing equations and briefly describes the two mixed-layer models adopted for the simulations. Section 3 discusses various aspects of the data set such as data processing, data selection, and the calculation of the heat and freshwater balance. Presented in Sections 4 and 5 are the results obtained from the simulations for the periods 1969-1971 and 1964-1965, respectively. Following this, in Section 6, is a discussion of the relative importance of the surface heat flux and stratification. Lastly, Section 7 summarizes our findings and offers some concluding remarks.

## Mixed-layer models

Many mixed-layer model inter-comparisons and calibrations have been carried out in the past 30 years (see [4] for a recent review). In this work, two representative models, a turbulence closure model and a bulk model, are used. While both types of models can adequately simulate the mixed-layer depth and temperature, both have shortcomings. Turbulence closure models tend to under-predict mixed-layer depths, and bulk models have adjustable parameters. To avoid model dependent errors and to check the consistency of the results, it is necessary to use different types of models as was done in other mixed-layer studies (e.g. [1]-[2]). No attempt was made to repeat the model inter-comparison exercises made by previous investigators with a different data set.

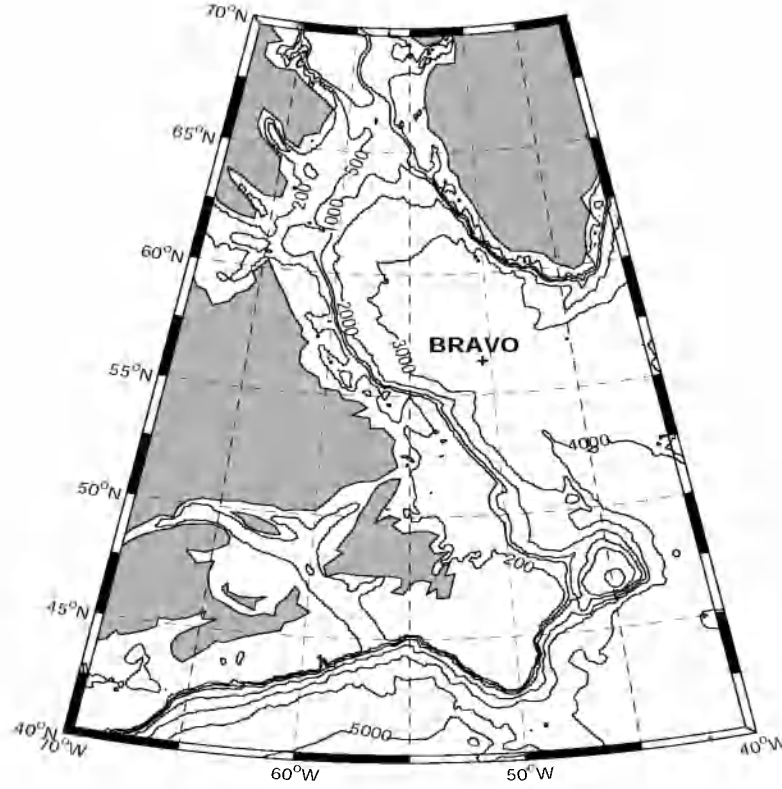


**Figure 2:** The location and local bathymetry of OWS Bravo.

The turbulence closure model used in this paper is based on the model of D'Alessio et al. [3]. The closure scheme in the model is only slightly different from the popular Mellor-Yamada formulation [5]. The mixed-layer depth is somewhat dependent on the definition used to compute it. Here, it is computed based on the level of turbulence present. It is defined as the depth at which the TKE drops below  $10^{-6} \text{ m}^2 \text{ s}^{-2}$ . The length scale,  $l$ , adopted is the Blackadar formula [6]:

$$l = \frac{\kappa(|z| + z_0)}{1 + \frac{\kappa|z|}{I_0}}, \quad (1)$$

with

$$\frac{1}{I_0} = \frac{1}{I_{MY}} + \frac{1}{I_b},$$

for locally stable conditions and  $I_0 = I_{MY}$  for locally unstable conditions. Here,  $I_{MY}$  is the Mellor-Yamada asymptotic length scale,  $I_b$  is the buoyancy length scale, and  $\kappa$  is the von Karmen constant. The dissipation of TKE is modeled according to Kolmogorov [7].

The bulk mixed-layer model used in this study is based on the formulation of Niiler and Kraus [8], Elsberry et al. [9] and Gaspar [2]. During deepening, the entrainment velocity is governed by

$$w_e = \frac{2}{h\Delta b} \left\{ mu_*^3 \exp\left(-\frac{h}{\lambda}\right) + \frac{1}{4} h[(1+n)B_0 - (1-n)|B_0|] \right\}, \quad (2)$$

where  $h$  is the mixed-layer depth,  $\Delta b$  is the buoyancy jump across the base of the mixed layer,  $u_*$  is the friction velocity,  $B_0$  is the buoyancy flux at the surface modified by short-wave radiation,  $\lambda = \frac{\kappa u_*}{f}$  is the Ekman length scale, and  $m$  and  $n$  are adjustable parameters. Gaspar [2] used a value of 1 for  $m$  while Oberhuber [10] used a value of 0.4.

If  $w_e$  is zero, mixed-layer deepening ceases and its depth is determined by solving the algebraic equation  $w_e = 0$ .

## Bravo data

Ocean weatherstation Bravo is located in the center of the Labrador Sea gyre (56.5° N, 51°W) and was maintained by the U.S. Coast Guard. During the period 1964-1974, surface meteorological measurements were routinely recorded as well as subsurface temperature and salinity profiles.

## Ocean data

The temperature and salinity data were retrieved from the Atlantic Fisheries Adjustment Program (AFAP) database at the Bedford Institute of Oceanography. This database includes hydrographic data from the northwestern North Atlantic, and represents a compilation of a variety of sources dating back to 1910. The majority of the temperature / salinity profiles at the Bravo site were taken between 1964 and 1974 when OWS Bravo was in operation. The number of profiles total over 2000. A description of the data can be found in Lazier [11]. The average sampling frequency over this period was approximately 15 profiles per month with a maximum of 79 profiles taken in August 1969. The depths and depth intervals were not fixed. The intervals vary from 5 m near the surface to 50 m at mid-depth. The large intervals are a major source of uncertainty in the determination of the mixed-layer depth during winter and spring.

## Atmospheric data and calculation of surface fluxes

Surface meteorological data taken by ship at 3 hour intervals from 1964-1974 included 20-m wind, 10-m air temperature, and 10-m dew-point temperature. Missing data were specified using linear interpolation. Surface downward short and long-wave radiation and precipitation rates were taken from the NCEP-NCAR 40-year reanalysis project (Kalnay *et al.* [12]). These data were linearly interpolated from 6 to 3 hour intervals.

From the meteorological data and modeled SST, the wind stress, sensible heat, and latent heat were calculated. The drag coefficient and sensible heat coefficient were calculated from the 20-m wind speed and the 10-m air-sea surface temperature difference using the method of Smith [13]. The latent heat coefficient was set to 1.2 times the sensible heat coefficient (Smith and Dobson [14]). The absorbed short-wave radiation at the sea surface was calculated by applying a constant albedo of 0.1 to the NCEP/NCAR downward short-wave radiation. The upward long-wave radiation at the surface was calculated by treating the sea surface as a black body having an emissivity of 0.97. The calculated upward long wave and NCEP/NCAR downward long wave were added to get the net surface long-wave heat.

There are other bulk formulas for computing sensible and latent heat fluxes, for example, algorithms based on COARE in the tropical Pacific (Fairall *et al.* [15]), and many formulas for short- and long-wave radiation. Global data sets for heat fluxes are also available (e.g., Josey *et al.* [16]). Since the precipitation data from NCEP/NCAR may have large uncertainties, we were

careful in our use of this data. In this study, the precipitation data were only used in a test run (see Section 4.1, Run 1) and in the salt balance calculation (Section 3.5).

A critical evaluation of the various bulk formulas and data sets is beyond the scope of this investigation. The adopted approach in this study was to use well-recognized methods to calculate the heat fluxes, and to check the results against previous heat flux studies at Bravo (Smith and Dobson [14]) in order to ensure that the heat fluxes we used were reliable. These same heat fluxes were then applied to the mixed-layer models under different oceanographic conditions. The focus is on the differences in the mixed-layer temperature and depths from the simulations, and not in the actual simulated values.

### Selection of simulation periods

The selection of the simulation periods was based on the consideration of both data quality and oceanographic features. Between 1964 and 1974, 20% of the ship meteorological data were missing. The simulation periods were selected by finding the longest periods with the least missing meteorological data that exhibited interesting oceanographic features. Two periods were chosen, 1964-1965 and 1969-1971. These periods had a data loss of only 1.4% and 2.5%, respectively. The period 1964-1965 represents an interval with normal oceanographic conditions for the Labrador Sea, whereas the period 1969-1971 is characterized as one having a very low salinity. A more detailed description of the oceanographic conditions in the Labrador Sea for these two periods is given in Section 4.

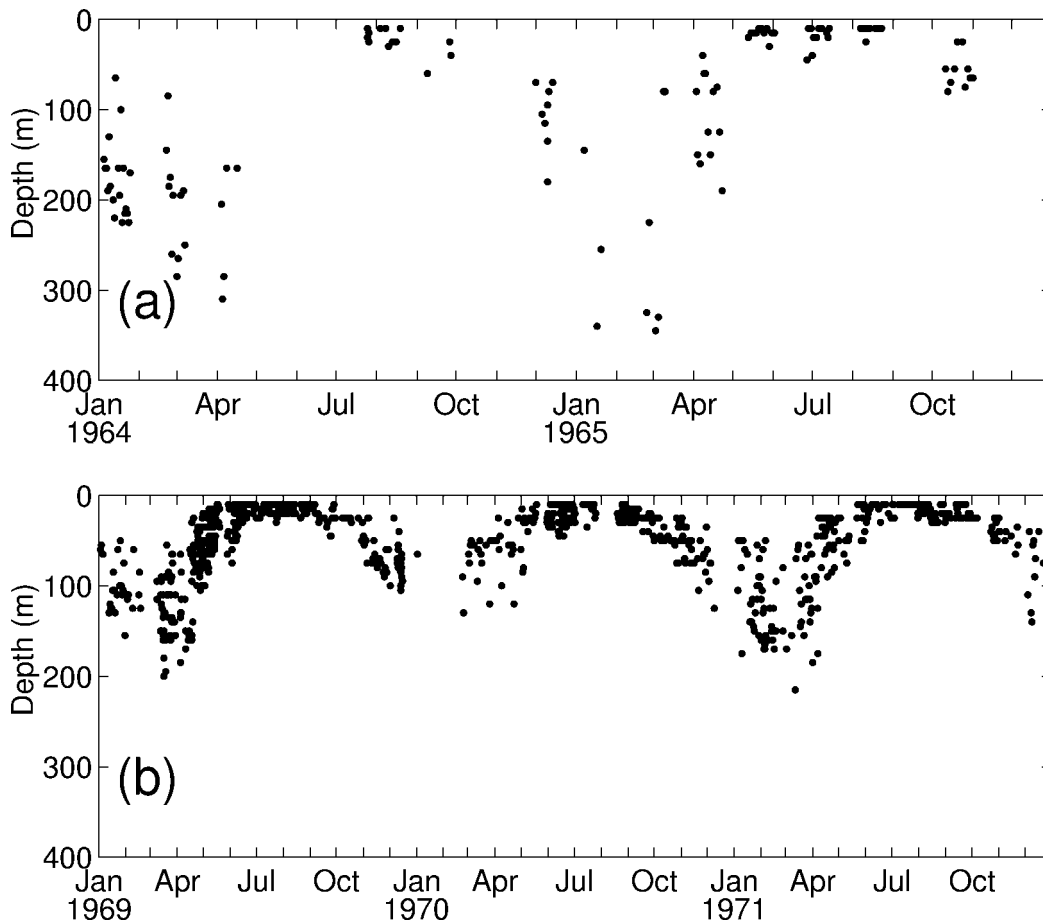


**Figure 3:** Mixed-layer depth determined from the data. (a): Period 1964-1965. (b): Period 1969-1971.

### Determination of mixed-layer depth from the data

The mixed-layer depth is defined as the depth at which the density changes by  $0.02 \text{ kg m}^{-3}$  from the surface density. This tolerance level was established by trial and error and by manually examining each profile to ensure that the depth determined by this method was reasonable. The varying depth intervals of the data points yield uncertainties of up to 25 m. Plotted in Figure 2 is the time variation of the mixed-layer depth for the two periods considered in this study. In previous studies, such as Martin [1] and D'Alessio *et al.* [3], which employed data from the Pacific stations November and Papa, the mixed-layer depth was defined as the depth at which the temperature changes by  $0.1^\circ\text{C}$  from the sea-surface value. In the absence of salinity measurements this proved to be a reasonable method for determining the mixed-layer depth.

Figure 3 shows that the winter mixed-layer depth during the two periods varies between 150 m and 350 m. This is consistent with the direct measurements of sub-surface floats during the winter of 1996-1997, which indicated that mixed layers deeper than 800 m were concentrated in the area about 200 km west of Bravo. Shallower mixed layers were found north of  $60^\circ\text{N}$  and southwest of the southern tip of Greenland. In the vicinity of Bravo, the mixed-layer depths were in the range 0 – 400 m (Lavender *et al.* [17]).

### Heat and salt balance

The basic assumptions made in one-dimensional, mixed-layer models are that horizontal advection is negligible, and that changes in the mixed-layer are driven mainly by air-sea fluxes. An analysis of the heat and salt budgets at Bravo, similar to that adopted by Abdella and D'Alessio [18], can provide verification regarding the validity of these assumptions, as well as the reliability of the data and air-sea flux calculations. If the balance does not hold within expected errors, then one-dimensional, mixed-layer model simulations are meaningless.

The temperature and salinity balance in the upper ocean from a fixed depth,  $D$ , below the maximum mixed-layer depth to the surface is given by

$$\frac{d}{dt} \int_{-D}^0 \bar{T} dz = \frac{1}{\rho_0 c_p} [Q + I_0], \quad (3)$$

$$\frac{d}{dt} \int_{-D}^0 \bar{S} dz = -\bar{S}_0 [P - E], \quad (4)$$

where  $Q$  is the sum of sensible heat, latent heat, and long-wave radiation,  $\bar{S}_0$  is the surface salinity,  $P$  and  $E$  are the precipitation and evaporation rates, respectively and  $I$  denotes the short-wave radiation with the subscript 0 referring to the value at the sea surface ( $z=0$ ). The adopted sign convention is that  $Q$  is positive for heating and negative for cooling. To arrive at the above results, we have made the assumption that  $w_e$ ,  $I$ ,  $\bar{T}' w'$ , and  $\bar{S}' w'$  vanish at  $z = -D$ . As gaps between oceanographic measurements are sometimes quite large, the errors in computing the left-hand sides of equations (3) and (4) may be large. To circumvent this potential problem, we integrate these equations in time to obtain an alternate form for the balance equations:

$$\int_{-D}^0 \bar{T}(t) dz - \int_{-D}^0 \bar{T}(t=0) dz = \frac{1}{\rho_0 c_p} \int_0^t [Q + I_0] dt, \quad (5)$$

$$\int_{-D}^0 \bar{S}(t) dz - \int_{-D}^0 \bar{S}(t=0) dz = -\bar{S}_0 \int_0^t [P - E_0] dt. \quad (6)$$

The left-hand sides represent changes in the heat and salt content at a given time, and can be calculated from each individual profile. Figures 4 and 5 are plots of the two sides of (5) and (6) for the periods 1964-1965 and 1969-1971, respectively. Here,  $D$  was taken to be 500 m for the first period and 300 m for the second period as suggested from Figure 3. The temperature and salinity used on the left-hand sides of the equations were monthly averages. The sea-surface temperatures used in the heat flux calculation of the right-hand sides were the averages of the top 10 m interpolated to 3-hourly intervals.

From January 1964 to January 1965 in Figure 3 and from January 1969 to July 1970 in Figure 5, the agreement between the left and right-hand sides of (5), as indicated by solid circles and solid curves, respectively, is reasonably good. However, during the following month and a half in each period, the differences become large and thus, suggest that the heat is not balanced during these two short periods. The reason for this is difficult to determine. Errors in the meteorological and ocean data, along with strong advection are possible explanations. Gaspar (1988) found a similar short-term imbalance in the OWS Papa data and speculated that the imbalance had an advective origin.

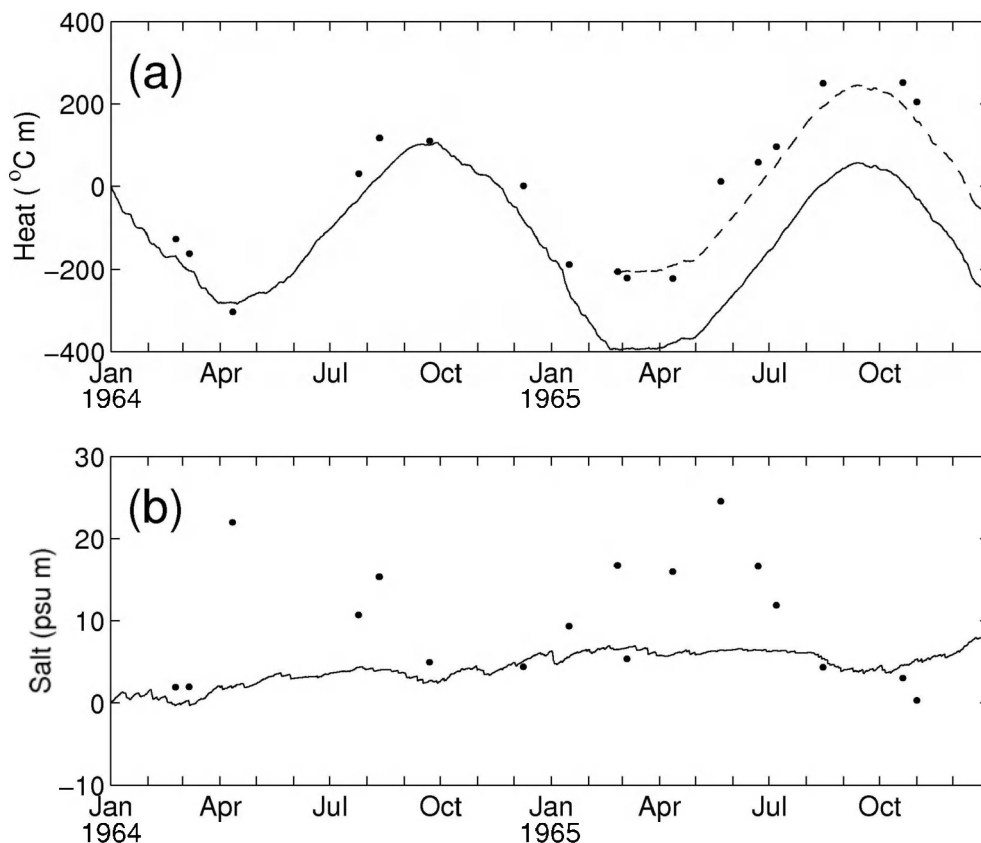


**Figure 4:** The heat and salt balances for the period 1964-1965. (a): The left-hand (solid circles) and right-hand side (solid line) of equation (5). (b): The left-hand (solid circles) and right-hand side (solid line) of equation (6). The dashed line represents the shifted curve due to changing the start time from January 1964 to February 1965.

During the remaining time intervals in the two periods, the curves were vertically shifted to coincide with the solid dot on February 1965 in Figure 4 and on October 1970 in Figure 5. This has the effect of re-establishing the heat balance. The shifting is equivalent to changing the start



time in equation (5) from the start of the data to February 1965 and October 1970 for the two periods, respectively. The results show that except for about a month and a half in each period, the temperature conservation equation approximately holds. This implies that our heat flux calculations are reliable and justifies the use of the one-dimensional mixed-layer models. In the simulations presented in the following sections, we skip the two short one and a half month periods during which heat is not balanced, and re-initialize the temperature profiles on February 1965 and October 1970.

Figures 4 and 5 show clearly that the salt balance is violated. This imbalance can be caused by errors in the precipitation data and the neglect of salinity advection in the analysis. The salt balance in the central Labrador Sea has been studied by Khatiwala *et al.* [19]. They found that horizontal advection is the dominant process controlling the salt balance. For both salinity and temperature, the importance of the vertical processes versus advection depend on the relative magnitudes of the source term (heat fluxes, P-E) and the advection term in the respective equations. Our calculations indicate that the source term dominates the temperature equation, while the combination of salt advection and uncertainties in the source term (P-E) invalidates the one-dimensional salt conservation equation.

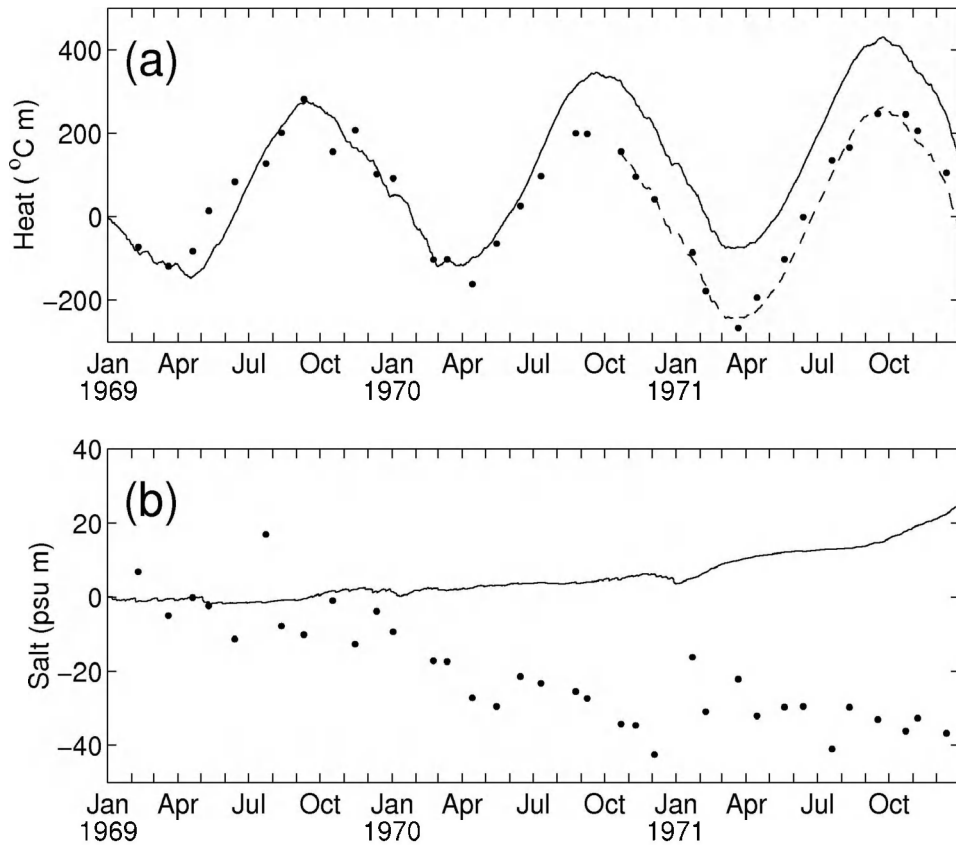


**Figure 5:** The heat and salt balances for the period 1969-1971. (a): The left-hand (solid circles) and right-hand side (solid line) of equation (5). (b): The left-hand (solid circles) and right-hand side (solid line) of equation (6). The dashed line represents the shifted curve due to changing the start time from January 1969 to October 1970.

To summarize, the calculations in this section indicate that one-dimensional mixed-layer models cannot be expected to simulate salinity well at Bravo. In this paper, we will therefore not attempt to simulate the salinity change at Bravo, except for a test run for comparison purposes (see Section 4.1).

### Effects of salinity on model simulations

Model results for the two selected periods: (a) 1964 - 1965 and (b) 1969 - 1971 will be presented separately. Period (a) represents a period having normal oceanographic conditions for the central Labrador Sea. The maximum mixed-layer depth is about 300 m (Figure 3) and the surface salinity has a mean value of 34.8 psu with a small seasonal variation. Starting in 1967, the salinity of the upper ocean decreased steadily reaching a minimum of 33.5 psu in the fall of 1971. This period is referred to as the Great Salinity Anomaly (Belkin et al. [20]). The freshening of the Labrador Sea can result in a highly stratified upper ocean and a shallow mixed layer. Period (b) encompasses the last three years of the low salinity period. The data in period (a) has large gaps ranging from one to three months, and thus a quantitative comparison of model errors is not feasible. Our effort in the analysis of model simulations is therefore concentrated on period (b).

For both periods, the mixed-layer models were numerically integrated in time using the observed temperature profile at the beginning of each period as the initial condition. The salinity, on the other hand, was either prescribed for the entire simulation or was initially specified using the observed salinity profile. Both the bulk model and the turbulence closure model used a 15-minute time step with linear interpolation used to generate data between the observed 3-hourly measurements. The vertical resolution used in the models was 1 m.

In the following simulations the bulk model was run with  $n = 0.2$ ,  $m = 0.8$  and  $\bullet = 0.4$ . These values were obtained from test runs that were carried out to achieve good agreement with the observations, and were used during both periods. Both models ran with an ambient, or background, diffusivity of  $K_v = 0$  and exhibited negligible sensitivity to  $K_v$ . This will be discussed in more detail in Section 4.2. Table 1 gives the relevant information about the runs to be discussed in the following sub-sections.

**Table 1:** Table of Runs performed indicating the period, salinity specification, air temperature, water type and corresponding figures for each simulation.

Period	Run	Salinity	Air temperature	Figure
1969 to 1971	1	Calculated	Ta (data)	6
	2	Monthly Mean (data)	Ta (data)	7, 8, 9
	3	Climatology	Ta (data)	11
	4	Monthly Mean (data)	Ta (data) - 4°	13
1964 to 1965	5	Monthly Mean (data)	Ta (data)	12
	6	Monthly Mean (data)	Ta (data) + 2.25°	14

**Salinity calculated from the models - Run 1**

The calculation of the salt budget in the previous section indicates that the model assumptions and the data are not compatible. Consequently, the model is not expected to reproduce the observed mixed-layer salinity. Despite this, a simulation that computed salinity from the salinity equation using the initial observed salinity profile was conducted. The purpose of this is to demonstrate that, by comparison with the results of sub-section 4.2, the optimum way to simulate the sea-surface temperature and mixed-layer depth is to use the observed salinity, not the climatological salinity, in the mixed-layer models.

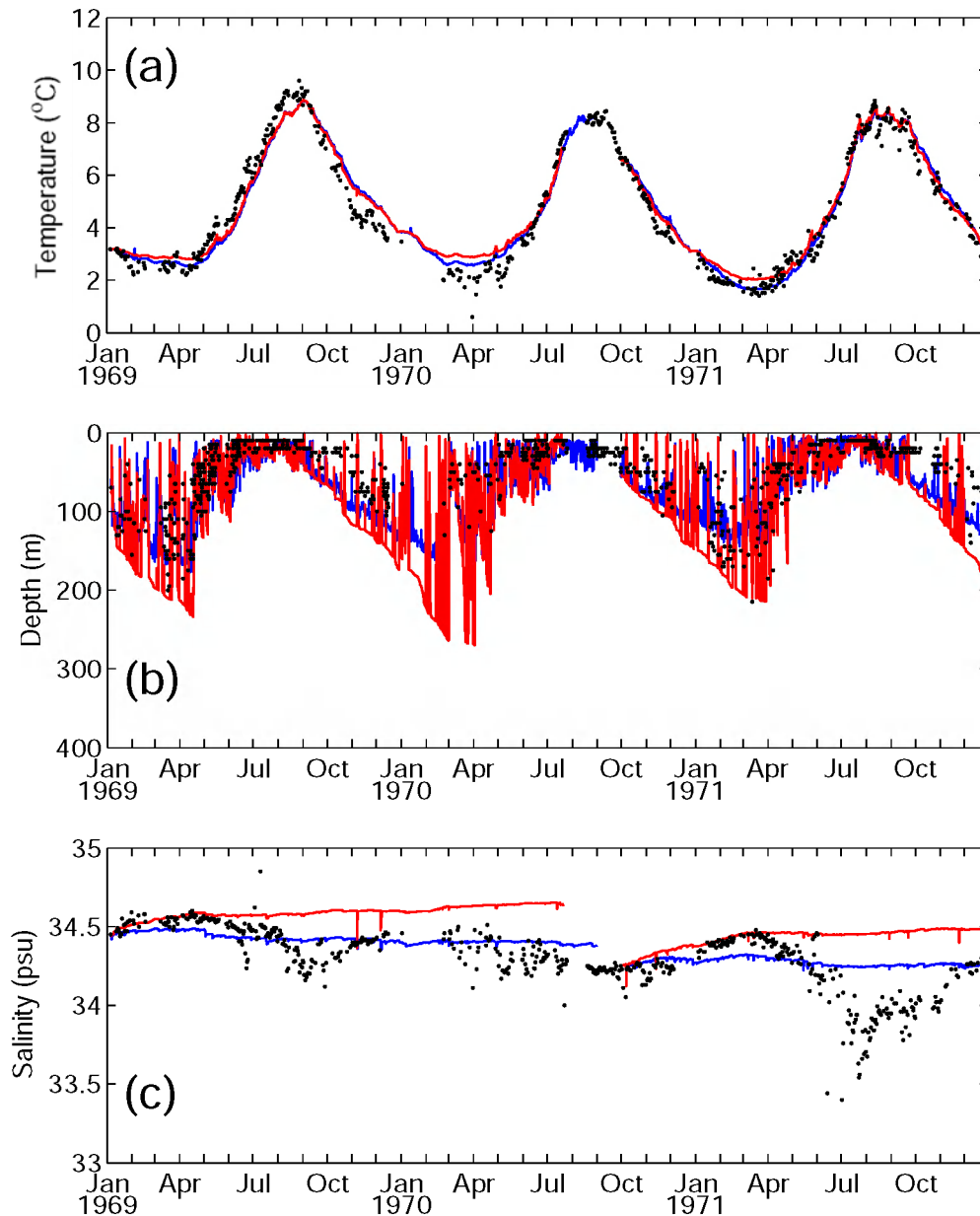


**Figure 6:** Comparison of (a) modeled and observed sea-surface temperature; (b) modeled mixed-layer depth; (c) modeled and observed sea-surface salinity from Run 1. Red: Bulk model. Blue: Turbulence closure model. The solid circles represent observed temperatures, salinities, and mixed-layer depths.

In Run 1, observed temperature and salinity profiles having well-defined mixed-layer depths in January 1969 were used as initial conditions for the model. The model was re-initialized with profiles on October 1970 to re-balance the heat budget as previously explained. Figures 6a,b,c show the time evolution of the mixed-layer temperature, depth, and salinity, respectively.

The modeled mixed-layer depth as computed by the bulk model reaches depths of 220 – 280 m in March – April, which is about 80 m greater than the observed depth. The temperature simulation is reasonably good except during the spring period. In March – April, when the temperature is at its minimum, the modeled temperature is 1°C to 2°C too high. The high temperature is caused by excessive entrainment of the deeper warm water into the mixed layer. The modeled salinity deviates substantially from the observed salinity as expected. The over-prediction of the maximum mixed-layer depth is a common feature of bulk mixed-layer models (Martin [1]). Adjusting the values of  $\kappa$  and  $n$  can make the mixed layer shallower, but not by 80 m.

The turbulence closure model, on the other hand, under-predicts the mixed-layer depth. Apart from a spike in March 1970, the maximum mixed-layer depth is about 175 m. This is also a common feature associated with the Mellor-Yamada type models and is also pointed out by Martin [1]. The temperature simulation appears to be somewhat better than that of the bulk model.

### Salinity from data - Runs 2 and 3

In Run 2 (Figure 7), salinity was prescribed. The values used were the monthly averaged salinity data from the simulation period. For the bulk model, the modeled temperature agrees well with the data. The maximum mixed-layer depth is 180 m, which is slightly less than the observed depth of 200 m. For the turbulence closure model, the simulated SST is very similar to that of the bulk model, but the mixed-layer depth is shallower. It was noted earlier in the paper that the mixed-layer depth in the turbulence closure model and in the Bravo data is not accurately defined. Therefore, model-data comparisons should focus on the SST and the difference in mixed-layer depth between the runs and the models.

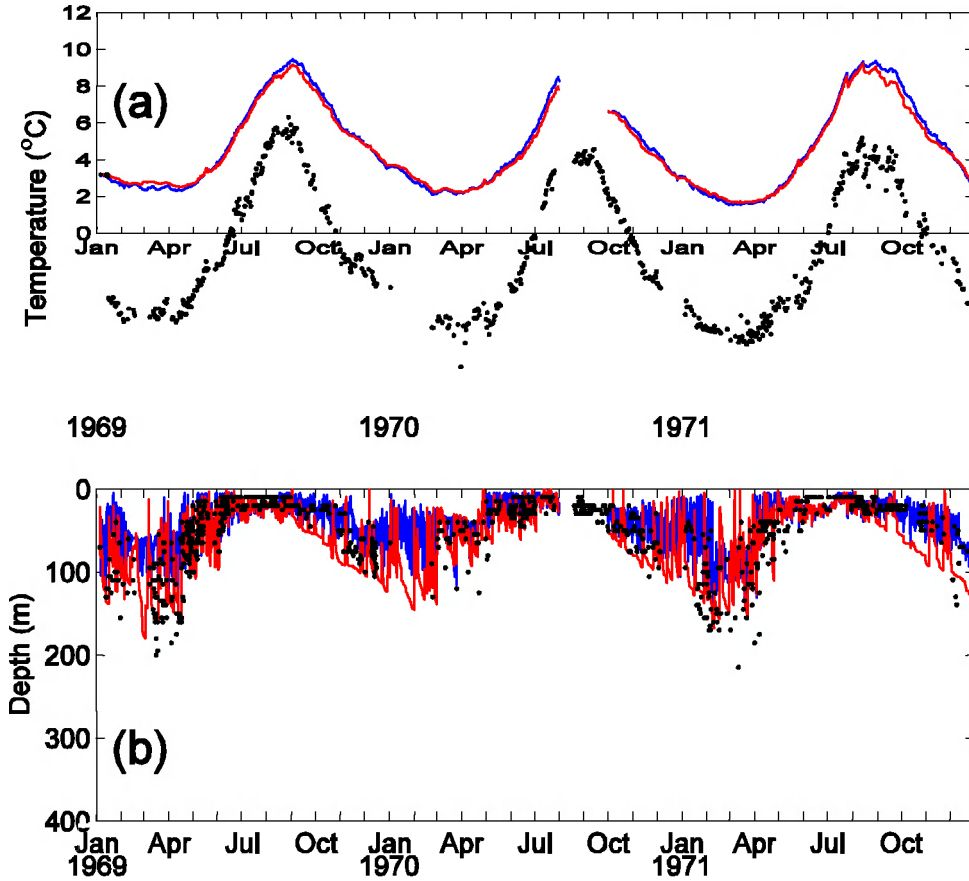
Plotted in Figure 8 is the monthly mean temperature difference between the models and the data for Run 2. Both models show similar patterns in the errors. The temperature is overestimated in the fall and underestimated in the spring of 1969 and 1971. The errors appear to be random during 1970 though. For the bulk model the maximum error is about 0.7°C, while for the turbulence closure model the maximum error is about 1°C.

Figure 9 shows the temperature in the depth-time plane from the monthly-averaged data and model simulations of Run 2. All the major features of the temperature field below the surface are reproduced in the models and the differences between the two models are not significant. The model results show uniform or near-uniform temperature in the mixed layer, most conspicuously during the winter months, while in the data the temperature field has large vertical gradients. This is due to the fact that the data values are averages of many profiles from observations.

Run 2 can be considered as a diagnostic calculation in the sense that one of the model variables is derived from the data as opposed to being predicted or prescribed using climatological data available from independent sources.

Sensitivity studies for several model parameters were conducted with the salinity field specified as in Run 2. In one simulation where  $\kappa$  in the bulk model was changed from 0.4 to 1, the maximum mixed-layer depth increased by 40 m, and the mixed-layer temperature remained about the same. In another run, the background diffusivity used to re-stratify the water below the mixed layer was set to  $0.0001 \text{ m}^2 \text{ s}^{-1}$ . This had little effect on the mixed-layer depth. The mean mixed-layer temperature increased by 0.1°C. These changes are considered relatively small. The background diffusivity improves the temperature and salinity structure below the mixed layer by re-stratifying the cold and low salinity water brought to the maximum mixed-layer depth by deepening. The water optical type was also changed from Very Clear to the more turbid Type I

(Paulson and Simpson [21]). The maximum temperature difference was higher than that in Run 2 by almost  $2^{\circ}\text{C}$ . But the cooling period showed little sensitivity to the water optical type since solar radiation does not penetrate to great depths.



**Figure 7:** Comparison of (a) modeled and observed sea-surface temperature; (b) modeled mixed-layer depth from Run 2. Red: Bulk model. Blue: Turbulence closure model. The solid circles represent observed temperatures and mixed-layer depths.

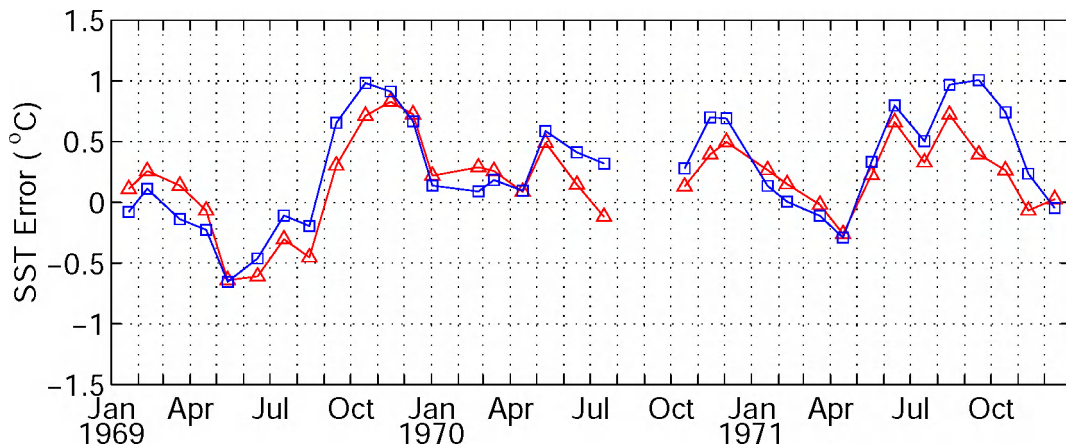


**Figure 8:** Difference between modeled and observed monthly-averaged sea-surface temperature. Red: Bulk model. Blue: Turbulence closure model.

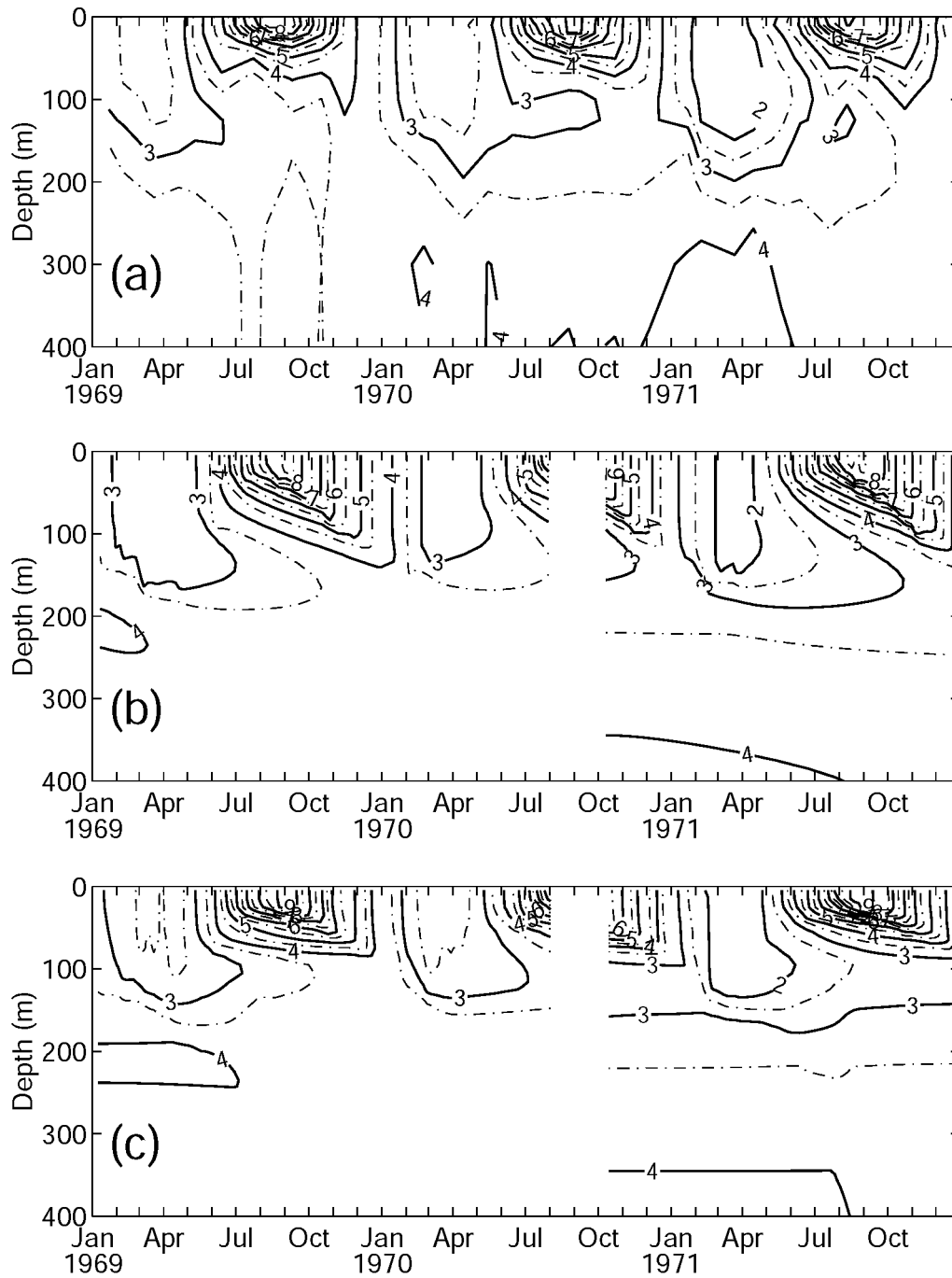


**Figure 9:** Contour plots of monthly-averaged temperature from (a) the data; (b) the bulk model, and (c) the turbulence closure model from Run 2.

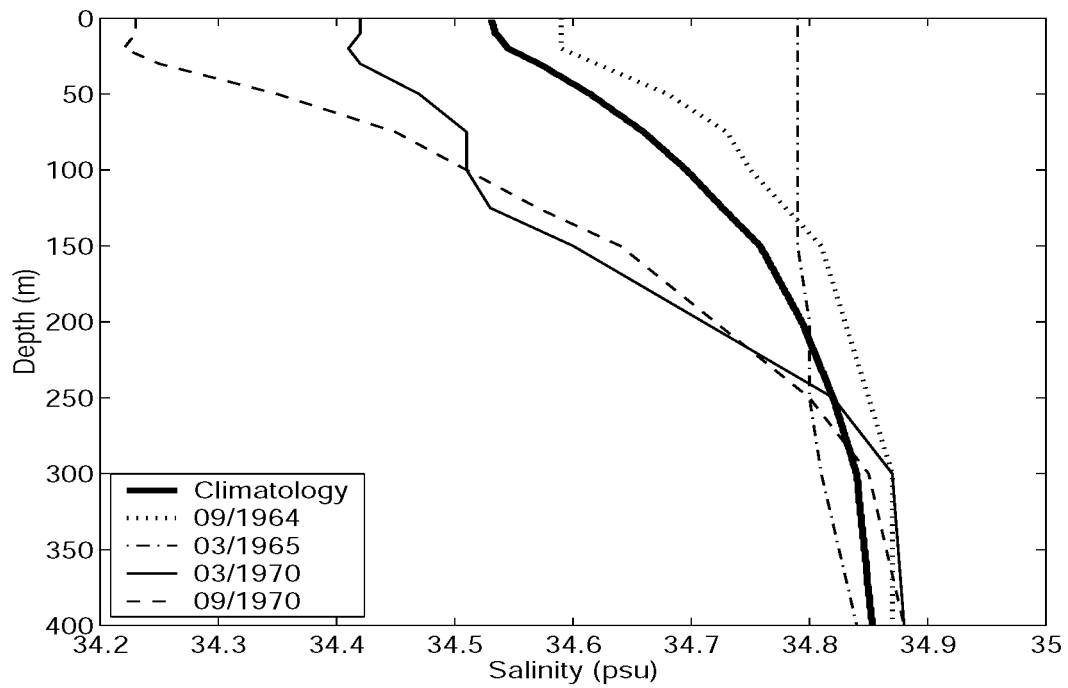


**Figure 10:** Comparison of climatological and selected monthly mean salinity profiles.

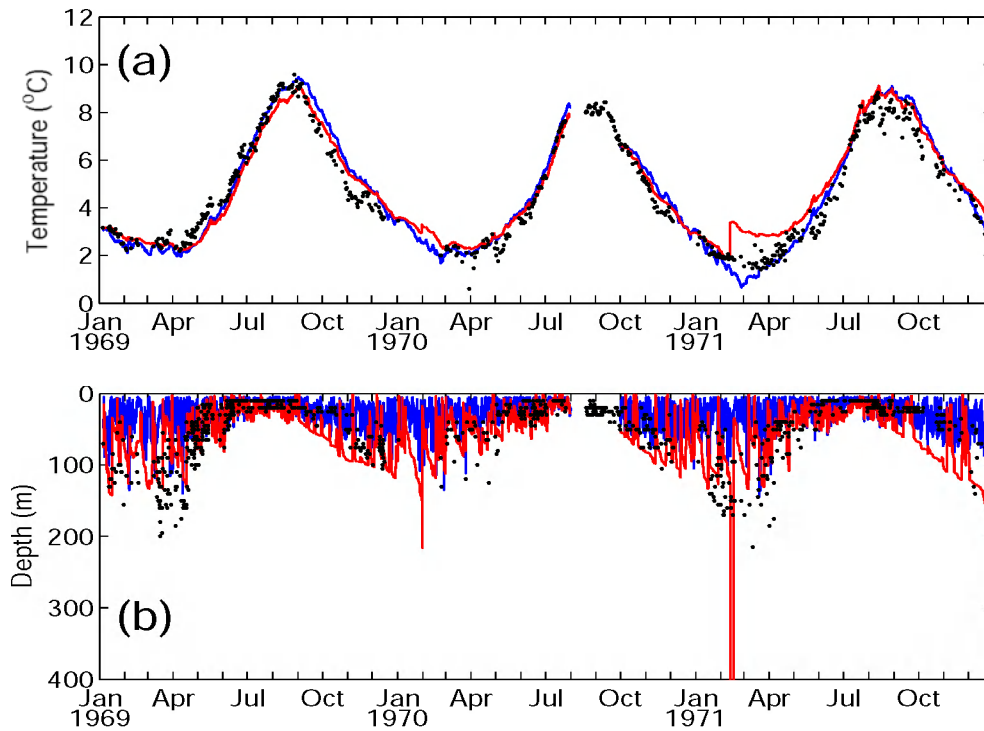


**Figure 11:** Comparison of (a) modeled and observed sea-surface temperature; (b) modeled mixed-layer depth from Run 3. Red: Bulk model. Blue: Turbulence closure model. The solid circles represent observed temperatures and mixed-layer depths.

### Salinity set to climatological mean - Run 3

In locations and periods where no ocean data are available, it is a common practice to use climatological data, usually produced from an objective analysis of observations, as a substitute. The climatological data may deviate substantially from the true temperature and salinity of the simulation period. To evaluate the sensitivity of the models to the uncertainty in the salinity specification, we compare model simulations using salinity from the climatology (Run 3) to that of observation (Run 2). The salinity climatology was produced by averaging salinity data at Bravo from 1928 to 1999 at each depth and was kept constant during the entire simulation. There are significant differences between the climatological salinity and the observed salinity as revealed in Figure 10. In the upper 250 m, the climatological salinity is higher than the observed salinity by as much as 0.35 psu during the period 1969-1971. The stratification in March 1970 is weaker than that shown in the climatological profile.

Using the turbulence closure model (Figure 11), a significant decrease in the mixed-layer depth occurs when compared to Run 2. The reason for this becomes evident from Figure 10, which shows the high-salinity water appearing at a shallower depth in the climatological data than that in the Bravo data. The shallower mixed-layer depth has a direct consequence on the simulated temperature. The minimum SST during February – March 1971 decreases considerably from that in Run 2 due to the smaller heat content associated with a shallower mixed layer.

Using the bulk model, the mixed-layer depth from Run 3 is smaller than that of Run 2 except during two short periods – February 1970 and February 1971. The large depths during these periods are the result of the high surface salinity and density (low stability) in Run 3 relative to the observed salinity in Run 2 (see Figure 10). A high density during the winter tends to make the water column unstable, and rapid deepening, which entrains the warmer deep water into the mixed layer, causes the mixed-layer temperature to increase, especially during February-April 1971. The different results from the two models suggest that the unrealistic salinity, i.e., climatology, is incompatible with the mixed-layer dynamics and the observed mixed-layer temperature, and hence should not be used to simulate the sea-surface temperature and mixed-layer depth at Bravo.

### Inter-annual change of the mixed-layer

The period 1964-1965 is a time when the Labrador Sea is subject to normal oceanographic conditions. The major difference between this period and 1969-1971, in terms of oceanographic conditions, is that the salinity in the upper 200 m during 1964-1965 is much higher than that during 1969-1971 (Figure 10). The mixed layer for 1964-1965 was simulated in Run 5. Here, the monthly mean salinity from the data was used as in Run 2. Figure 12 reveals that the March – April mixed-layer depths for the bulk model are about 300 m except for an isolated point in March 1964. This compares favorably with the observed depths shown in Figure 3, keeping in mind the uncertainty of 25 m in the data. More significant though, the predicted maximum mixed-layer depth is greater than that during the 1969-1971 period by 100 m, and is a major feature of the data. The greater depth is apparently related to salinity (more on this will be discussed in Section 6). The mean mixed-layer salinity during this period is higher than that of 1969-1971 by about 0.35 psu (Figure 10). The high salinity tends to destabilize the mixed layer and thus promotes convection. This explains the deeper mixed layer during the period 1964-1965. However, since a large surface heat flux can also create a deep mixed layer, the important question here is which factor is more important. This question will be addressed in the next section.

For the turbulence closure model, the March - April mixed-layer depths lie between 225 and 325 m. There is a short, isolated period in April 1964 when the mixed-layer depth exceeds 300 m. The maximum simulated mixed-layer depth during the 1964-1965 period is considerably deeper than that simulated during the 1969-1971 period. This difference is greater than 100 m but is in reasonable agreement with the bulk model. However, the maximum depths simulated by the



turbulence closure model over each of these periods is noticeably less than that predicted by the bulk model.

The simulated mixed-layer temperature agrees closely with observations for both models. The minimum mixed-layer temperature is approximately  $3^{\circ}\text{C}$ , which is about  $1^{\circ}\text{C}$  higher than the minimum temperature during the 1969 - 1971 period. The higher winter and fall temperatures are a result of the deeper mixed layer entraining warmer deep water into the mixed layer.

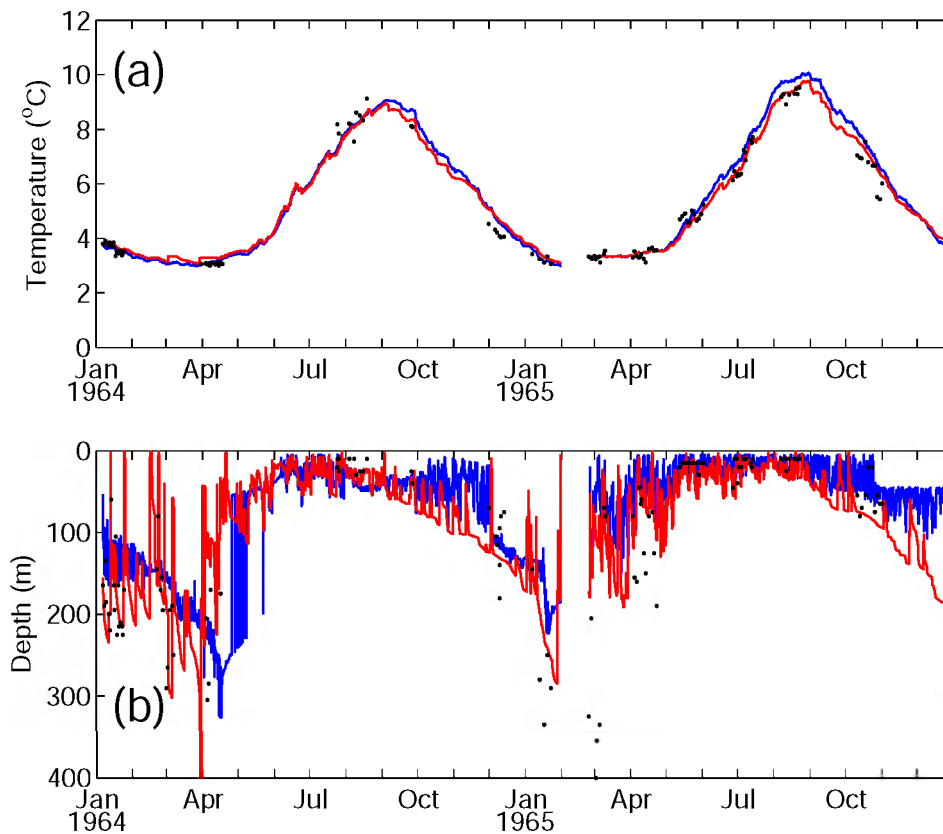


**Figure 12:** Comparison of (a) modeled and observed sea-surface temperature; (b) modeled mixed-layer depth from Run 5. Red: Bulk model. Blue: Turbulence closure model. The solid circles represent observed temperatures and mixed-layer depths.

### Stratification versus surface heat flux

Which factor is more important in the interannual variation of the mixed layer temperature and depth - stratification or surface heat flux? During the summer when the mixed layer is shallow, the surface heat flux and the optical properties of the water are the dominant factors as discussed in Section 4.2. The situation during the winter is less clear. The mean winter (December, January, February) surface heat loss is  $191 \text{ Wm}^{-2}$  during 1964-1965, and  $164 \text{ Wm}^{-2}$  during 1969-1971. But despite the larger heat loss during 1964-1965, the winter SST from those years is higher than the corresponding SST from 1969-1970 by  $1^{\circ}\text{C}$ . Apparently, the surface heat loss is not the major factor causing the SST difference between these two periods. The shallow mixed-layer during 1969-1971 can be due to small heat loss or low surface salinity or both.

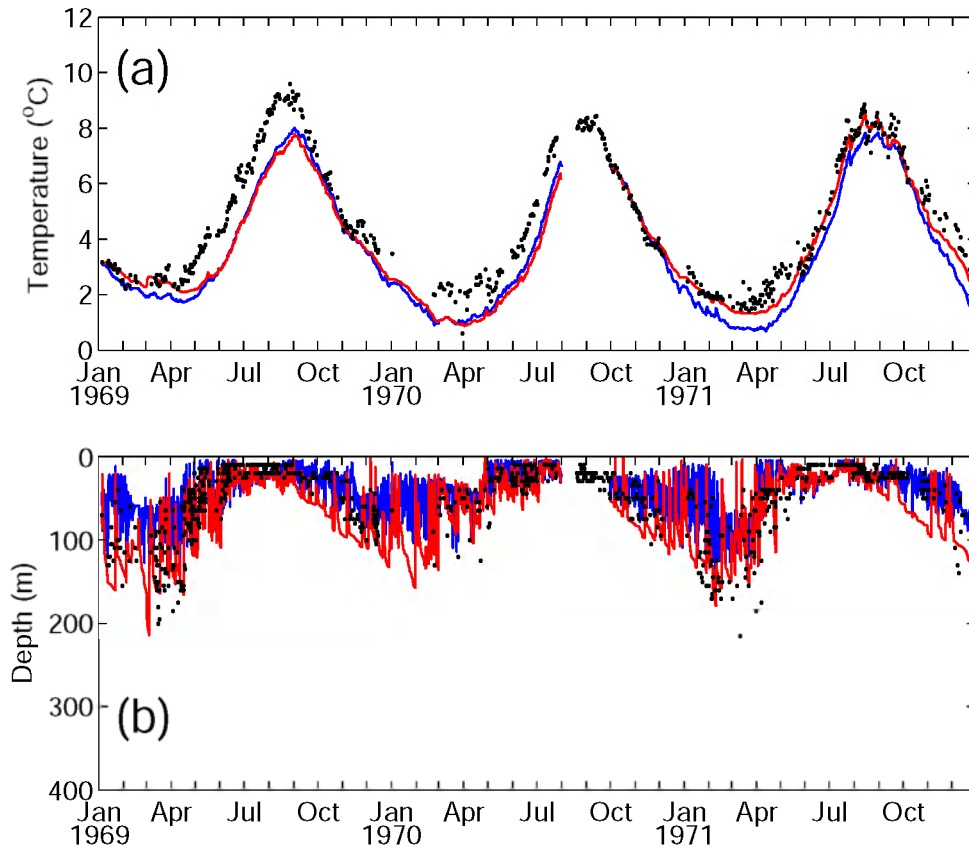


**Figure 13:** Comparison of (a) modeled and observed sea-surface temperature; (b) modeled mixed-layer depth from Run 4. Red: Bulk model. Blue: Turbulence closure model. The solid circles represent observed temperatures and mixed-layer depths.

To determine the factors that are responsible for the differences during the two periods, two additional model runs were conducted. In Run 4 (Figure 13), the air temperature for the 1969-1971 period was lowered by  $4^{\circ}\text{C}$ , resulting in a mean winter surface heat flux equal to that of the 1964-1965 period. The maximum mixed-layer depth is just slightly greater than that of Figure 7, but still much smaller than that of the 1964-1965 period (Figure 12). The minimum mixed-layer temperature is lower than that of Figure 8 by about  $1^{\circ}\text{C}$ . This suggests that, in comparison to the 1964-1965 period, the shallower mixed-layer depth during 1969-1970 is mainly due to the high stratification brought on by the low surface salinity.

In Run 6 (Figure 14), the air temperature for the 1964-1965 period was increased by  $2.25^{\circ}\text{C}$ , resulting in a mean winter surface flux equal to that of the 1969-1971 period. A comparison with Figure 11 shows that the mixed-layer depth is almost unchanged, and the temperature during the winter is higher than that of Figure 12 by only a fraction of a degree.

These model runs suggest that the difference in maximum (winter) mixed-layer depth between the two periods is mainly due to the difference in stratification, rather than the difference in surface heat flux. The winter mixed-layer temperature, however, depends on both stratification and surface heat flux. The dependence on the surface heat flux is weak for a deep mixed layer.

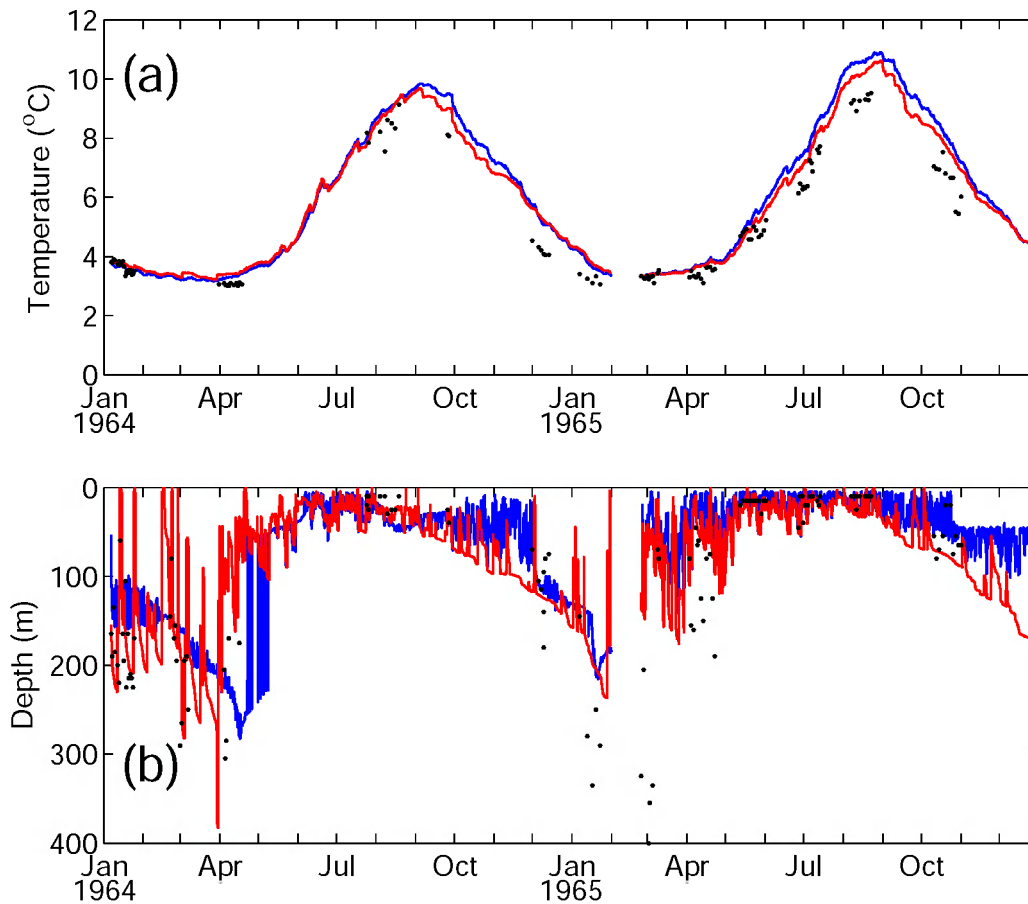


**Figure 14:** Comparison of (a) modeled and observed sea-surface temperature; (b) modeled mixed-layer depth from Run 6. Red: Bulk model. Blue: Turbulence closure model. The solid circles represent observed temperatures and mixed-layer depths.

## Conclusions

Presented in this paper is a study of the role of salinity in the variability of the upper ocean in the central Labrador Sea. Ocean data at OWS Bravo were simulated using a bulk mixed-layer model and a turbulence closure model over two representative periods: 1964-1965 and 1969-1971. Salinity cannot be simulated with the one-dimensional models because the salt balance at OWS Bravo is mainly controlled by the large-scale circulation of the Labrador Sea. By specifying the salinity in the models according to observations, good agreement between the simulated and observed sea-surface temperature can be obtained.

The sensitivity of the mixed-layer parameters to the salinity has been investigated by comparing model simulations using salinity data with simulations using time-independent climatological salinity profiles. The latter results in large errors in the sea-surface temperature and mixed-layer depth in both models during the cooling phase (winter and spring). This is due to the fact that the salinity climatology deviates substantially from the observed salinity during the simulation periods. The simulations demonstrate the importance of the correct specification of the salinity in mixed-layer models in high-latitude regions where the oceanographic and atmospheric conditions are similar to those at Bravo. The high sensitivity to the salinity is in contrast to the mixed-layers of the mid-latitude Pacific. The variation of surface salinity at OWS November has a similar

magnitude as that of Bravo (Figure 1), but the modeled mixed-layer depth and sea-surface temperature are not as sensitive to the way in which the salinity is specified or calculated in the models, as demonstrated by the simulations of Martin [1] and D'Alessio *et al.* [3] using the 1961 data. The main reason for this is that the density depends more strongly on the salinity in the high-latitude Atlantic than it does in the mid-latitude Pacific. During the heating phase (summer and fall), on the other hand, the sea-surface temperature is not sensitive to the salinity and depends mainly on the surface heat flux and the optical properties of the surface water because the mixed layer is shallow and short-wave radiation dominates the heat flux.

Since the surface heat flux, in general, is a major factor influencing the mixed-layer depth and temperature, we investigated the relative importance of the surface heat flux and salinity in the mixed-layer dynamics. During 1964-1965, a period of normal salinity, the maximum mixed-layer depth is 300 m and the corresponding SST is 3°C, which occur during March – April. In comparison, the same quantities during 1969-1971, a period marked by abnormally low salinity and relatively warm winters, are about 100 m shallower and 1°C lower. From model runs in which the air temperature was raised or lowered artificially so that the winter surface heat flux was the same during the two periods, we found that the salinity, and the stratification brought on by this, is mainly responsible for the difference in the mixed-layer depth between these two periods. The lower SST during 1969-1971 is the result of the smaller amount of warm ambient water entrained into the shallow mixed layer. The model simulations demonstrate that the salinity can be as important as the surface heat flux in controlling the interannual variation of the mixed-layer depth at OWS Bravo.

## Acknowledgments

S.J.D.D. wishes to acknowledge financial support from the Natural Sciences and Engineering Research Council of Canada. The work performed at BIO was supported by the Program for Energy Research and Development. The meteorological data from Bravo were provided by the British Oceanographic Data Centre.

## References

- [1] Martin, P.J., 1985: Simulation of the mixed layer at OWS November and Papa with several models. *J. Geophys. Res.*, **90**, pp. 903-916.
- [2] Gaspar, P., 1988, "Modeling the seasonal cycle of the upper ocean", *J. Phys. Oceanogr.*, pp. **18**, 161-180
- [3] D'Alessio, S.J.D., Abdella, K. and McFarlane, N.A., 1998, "A new second-order turbulence closure scheme for modelling the oceanic mixed layer", *J. Phys. Oceanogr.*, **28**, pp. 1624-1641.
- [4] Tang, C.L., McFarlane, N.A. and D'Alessio, S.J.D., 2002, "Boundary layer models for the ocean and the atmosphere", *Atmosphere-Ocean Interactions, Advances in Fluid Mechanics Series*, pp. 223-264. WIT Press, Southampton, UK.
- [5] Mellor, G.L. and Yamada, T., 1974 "A hierarchy of turbulence closure models for planetary boundary layers", *J. Atmos. Sci.*, **31**, pp. 1791-1806.
- [6] Blackadar, A.K., 1962, "The vertical distribution of wind and turbulent exchange in a neutral atmosphere", *J. Geophys. Res.*, **67**, pp. 3095-3102.
- [7] Kolmogorov, A.N., 1942, "The equation of turbulent motion in an incompressible fluid", *Izv. Akad. Nauk. SSSR, Ser. Phys.*, **6**, pp. 56-58.

- [8] Niiler, P.P. and Kraus, E.B., 1977, "One-dimensional models of the upper ocean", *Modelling and Prediction of the Upper Layers of the Ocean*. E.B. Kraus, Ed., Pergamon, pp. 143-172.
- [9] Elsberry, R., Fraim, T.S. and Trapnell Jr., R.N., 1976, "A mixed layer model of the oceanic thermal response to hurricanes", *J. Geophys. Res.*, **81**, pp. 1153-1161.
- [10] Oberhuber, J.M., 1993, "Simulation of the Atlantic circulation with a coupled sea ice-mixed layer-isopycnal general circulation model. Part I: Model description", *J. Phys. Oceanogr.*, **23**, pp. 808-829.
- [11] Lazier, J.R.N., 1980, "Oceanic conditions at ocean weather ship Bravo, 1964-1974", *Atmos. Ocean*, **18**, pp. 227-238.
- [12] Kalnay E. and co-authors, 1996, "The NCEP/NCAR 40-year reanalysis project", *Bull. Amer. Met. Soc.*, **77**, pp. 437-471.
- [13] Smith, S.D., 1988, "Coefficients for sea surface wind stress, heat flux, and wind profiles as a function of wind speed and temperature", *J. Geophys. Res.*, **93**, pp. 15467-15472.
- [14] Smith, S.D. and Dobson, F.W., 1984, "The heat budget at ocean weather station Bravo", *Atmos. Ocean*, **22**, pp. 1-22.
- [15] Fairall, C.W., E.F. Bradley, D.P. Rogers, J.B. Edson, G.S. Young, 1996, "Bulk parameterization of air-sea fluxes for TOGA COARE", *J. Geophys. Res.* 101, pp. 3747-3764.
- [16] Josey, S.A., E.C. Kent and P.K. Taylor, 1999, "Southampton Oceanography centre ocean-atmosphere heat, momentum and freshwater flux atlas. Southampton Oceanography centre Report, No. 6, 30 pp.
- [17] Lavender, K.L., R.E. Davis and W.B. Owens, 2002, "Observations of open-ocean deep convection in the Labrador Sea from subsurface floats", *J. Geophys. Res.*, **32**, pp. 511-526.
- [18] Abdella, K. and S.J.D. D'Alessio, 2003, "A parameterization of the roughness length for the air-sea interface in free convection", *Environ. Fluid Mech.*, **3**, pp. 55-77.
- [19] Khatiwala, S., Schlosser, P. and Visbeck, M., 2002, "Rates and mechanisms of water mass transformation in the Labrador Sea as inferred from tracer observations", *J. Phys. Oceanogr.*, **32**, pp. 666-686.
- [20] Belkin, I.M., Levitus, S., Antonov, J. and Malmber, S.-A., 1998, "Great Salinity anomalies in the North Atlantic", *Progress in Oceanography*, **41**, pp. 1-68.
- [21] Paulson, C.A. and Simpson, J.J., 1977, "Irradiance measurements in the upper ocean", *J. Phys. Oceanogr.*, **7**, pp. 952-956.